Covariabilities of Winter U.S. Precipitation and Pacific Sea Surface Temperatures

HUI WANG AND MINGFANG TING

Department of Atmospheric Sciences, University of Illinois, Urbana–Champaign, Urbana, Illinois

4 October 1999 and 8 May 2000

ABSTRACT

The variability of winter average U.S. precipitation displays strong geographical dependence with large variability in the southeastern and northwestern United States. The covariance of the U.S. winter mean precipitation with Pacific sea surface temperature (SST) is examined in this study using the singular value decomposition (SVD) method. The first SVD mode indicates the U.S. precipitation pattern that is associated with the tropical El Niño/La Niña SST variation, while the second and third SVD modes relate the precipitation variability in the Pacific Northwest and southeast that is associated with the North Pacific SST variation. About 45% of the U.S. precipitation variabilities is related to the Pacific SST anomalies, among which, 35% is related to the North Pacific SST and 10% is related to the tropical Pacific SST. Each SVD precipitation pattern is associated with well-organized 500-mb height and zonal mean zonal wind anomalies. It is shown that the North Pacific SST anomalies associated with the U.S. precipitation are primarily driven by extratropical atmospheric circulation anomalies.

1. Introduction

The relationship between wintertime continental U.S. precipitation and tropical Pacific sea surface temperature (SST) has received much attention in the past two decades. Ropelewski and Halpert (1986, 1989) found systematic winter precipitation anomalies over the southeast United States in association with the tropical El Niño–Southern Oscillation (ENSO) SST variations. Bunkers et al. (1996) has studied the El Niño/La Niña-related precipitation over the northern plains. Seasonal predictions of winter mean U.S. precipitation based on the tropical Pacific SST variations have also been attempted (Barnston 1994; Wang et al. 1999).

The link between variations in U.S. precipitation and tropical Pacific SST is a manifestation of the extratropical atmospheric response to the tropical SST forcing. In addition, extratropical circulation variability also depends on internal atmospheric processes in the extratropics and their interaction with the midlatitude oceans (Lau 1997). This can be seen in the precipitation field. For example, a study by Ting et al. (1996) shows that the winter average U.S. precipitation anomalies are related to both tropical Pacific SST variations and to fluctuations in the midlatitude zonal mean zonal flow, which are significantly correlated to the North Pacific SST variations. The evidence naturally poses one question; namely, how important are the tropical SST anomalies in determining the winter average U.S. precipitation pattern?

The winter average atmospheric circulation associated with the ENSO has been documented in many studies (e.g., Horel and Wallace 1981). The theoretical basis linking the extratropical circulation and tropical forcing is illustrated by Hoskins and Karoly (1981). GCM experiments (e.g., Lau 1985) have further demonstrated the extratropical atmospheric response to the tropical SST forcing. The U.S. precipitation variability associated with ENSO has also been identified (Ropelewski and Halpert 1986, 1989). In contrast, similar extratropical air–sea interactions are more complex and less understood. It is becoming increasingly clear that the North Pacific SST anomalies associated with ENSO are related to the oceanic response to the atmospheric circulation anomalies forced by the tropical SST pattern (Wallace and Jiang 1987; Lau and Nath 1994). There are large amounts of midlatitude SST variability that are independent of ENSO (Deser and Blackman 1995), however. Although a positive feedback is evident in extratropical air–sea interaction in coupled model experiments (Lau and Nath 1996), the nature of the atmospheric response to midlatitude SST remains uncertain (Lau 1997). Furthermore, less emphasis has been placed on the relationship between variations in U.S. precipitation and North Pacific SST.

The present study is aimed at establishing the associations between winter average U.S. precipitation and

Corresponding author address: Hui Wang, School of Earth and Atmospheric Sciences, Georgia Institute of Technology, 221 Bobby Dodd Way, Atlanta, GA 30332-0340.
E-mail: huiwang@eas.gatech.edu

Pacific SST anomalies using observational data. The primary concern is to identify the Pacific SST patterns that tend to occur simultaneously with the prominent U.S. precipitation anomalies. The causal relationship between the two, however, is beyond the scope of this study. The approach parallels Ting and Wang (1997, referred to as TW hereafter), in which the relations between summer U.S. precipitation and Pacific SST were examined.

2. Data and methods

The database used in this study are similar to those in TW, and consist of monthly mean U.S. precipitation, Pacific SST fields, Northern Hemisphere 500-mb height and sea level pressure (SLP), from 1950 to 1994. Winter seasonal means are obtained by averaging together the monthly means of December–January–February. An anomaly is defined as the deviation of the seasonal mean from its long-term average. The U.S. precipitation data are taken from the Global Historical Climatology Network (Vose et al. 1992) for 1950–90 and from the gridded hourly precipitation data base (Higgins et al. 1996) for 1991–94, and processed into a 2.5° × 2.5° grid. The Pacific SSTs (20°S–60°N) are the Reconstructed Reynolds Data (Smith et al. 1996) on a 2° × 2° grid. The 500-mb heights and the SLP are taken from the National Centers for Environmental Prediction operational analyses on a 2.5° lat × 5° long grid over the Northern Hemisphere from 20° to 90°N. A more detailed description of the data and their quality can be found in TW.

Two statistical methods are used, that is, the singular value decomposition (SVD; Bretherton et al. 1992; Wallace et al. 1992) and the linear regression. The former is able to objectively identify pairs of spatial patterns describing the maximum temporal covariance between two fields and the latter is used to obtain anomalies that are associated with the variation in a base time series.

3. Results

a. Variability of U.S. precipitation

The long-term winter average U.S. precipitation pattern is shown in Fig. 1a. The wettest regions are the Pacific Northwest and the Gulf Coast states. Rainfall rates of over 3 mm day^{-1} are found in the Pacific Northwest coastal regions that are strongly influenced by Pacific storms. The precipitation maximum in the southeast, on the other hand, is related to abundant moisture supply from the Gulf of Mexico. The northern and central plains are relatively dry in winter, receiving less than 1 mm day^{-1} precipitation on average. Figure 1b shows the standard deviation of winter average precipitation. In general, regions of large variability coincide with regions of large long-term average values. Maximum variability is observed in the Pacific Northwest coastal states (>2 mm day^{-1}). Other regions of large

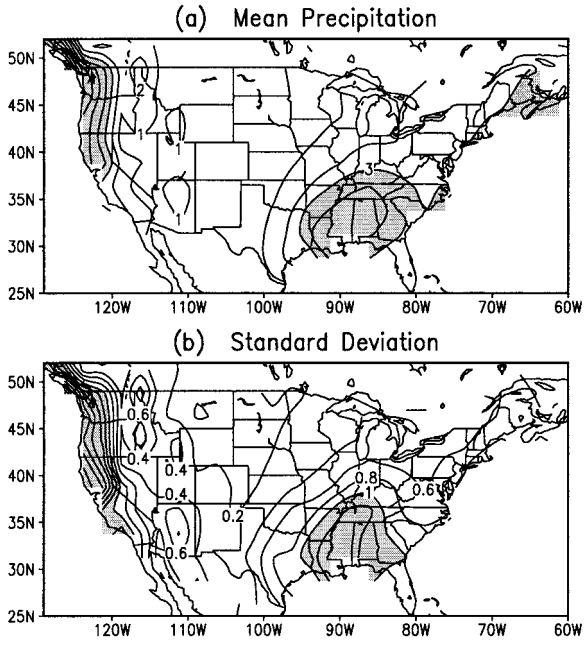

FIG. 1. Winter seasonal mean (a) and standard deviation (b) of U.S. precipitation. Contour intervals are 1 mm day^{-1} in (a) and 0.2 mm day^{-1} in (b). Values greater than 3 mm day^{-1} in (a) and greater than 1 mm day^{-1} in (b) are shaded.

standard deviations are found over the Gulf Coast states (>1 mm day^{-1}). The distribution of precipitation variability in Fig. 1b reflects the geographical dependence of winter precipitation on a seasonal timescale.

Both mean and anomalous U.S. precipitation show pronounced seasonality (TW). The regions with distinctive differences between cold and warm seasons are the West Coast and the Midwest. During winter, seasonal mean precipitation and its interannual variability is high along the West Coast, whereas in summer this signature shifts to the central plains (TW). In contrast, a broad area of large rainfall variability occurs in the southeast and along the East Coast during both seasons, associated with the inland penetration of moisture from the Gulf of Mexico and the western Atlantic. The seasonal dependence of the precipitation distribution and variability may suggest different relationships between U.S. precipitation and the Pacific SST during winter and summer.

b. Relations of U.S. precipitation to the Pacific SST

To examine the link between the U.S. precipitation and Pacific SST, the SVD analysis is performed by analyzing the covariance matrices of the two fields. The results are displayed using heterogeneous correlation patterns (Wallace et al. 1992). Table 1 lists the statistics for the first three SVD modes, including the percentage of squared covariance explained by each mode, the temporal correlation between pairs of expansion coefficients, and the variance in individual fields that are ex-

TABLE 1. Statistics of the leading SVD SST and precipitation modes.

	Squared covariance	Temporal correlation	SST variance	Precipitation variance
Mode 1	64%	0.77	48%	11%
Mode 2	16%	0.69	7%	24%
Mode 3	9%	0.71	7%	12%

plained by each mode. Together the three modes account for 89% of the squared covariance between the two fields, and the corresponding components explain 62% of the SST variance and 47% of the precipitation variance, respectively.

The first SVD mode explains 64% of the squared covariance between SST and precipitation. Its heterogeneous correlation patterns are shown in Figs. 2a and 2b for SST and precipitation, respectively. The SST pattern itself explains 48% of the total SST variance (Table 1). This mode is characterized by the El Niño SST pattern, with the large positive correlations in the eastern and central equatorial Pacific, negative correlations in the central North Pacific, and positive correlations along the coast of North America. The pattern is identical to the ENSO mode of Deser and Blackmon (1995). The first SVD mode of precipitation, which explains 11% of the total U.S. precipitation variance, has a well-defined pattern over the domain. Negative correlations are found in the northern plains and in the region extending from the Ohio River valley to the east of the Great Lakes. Positive correlations are found in the Gulf Coast states, the southern plains and the Southwest. This is the canonical precipitation pattern associated with El Niño that has been found in many previous studies (e.g., Ropelewski and Halpert 1986, 1989; Ting et al. 1996). Although this mode only explains

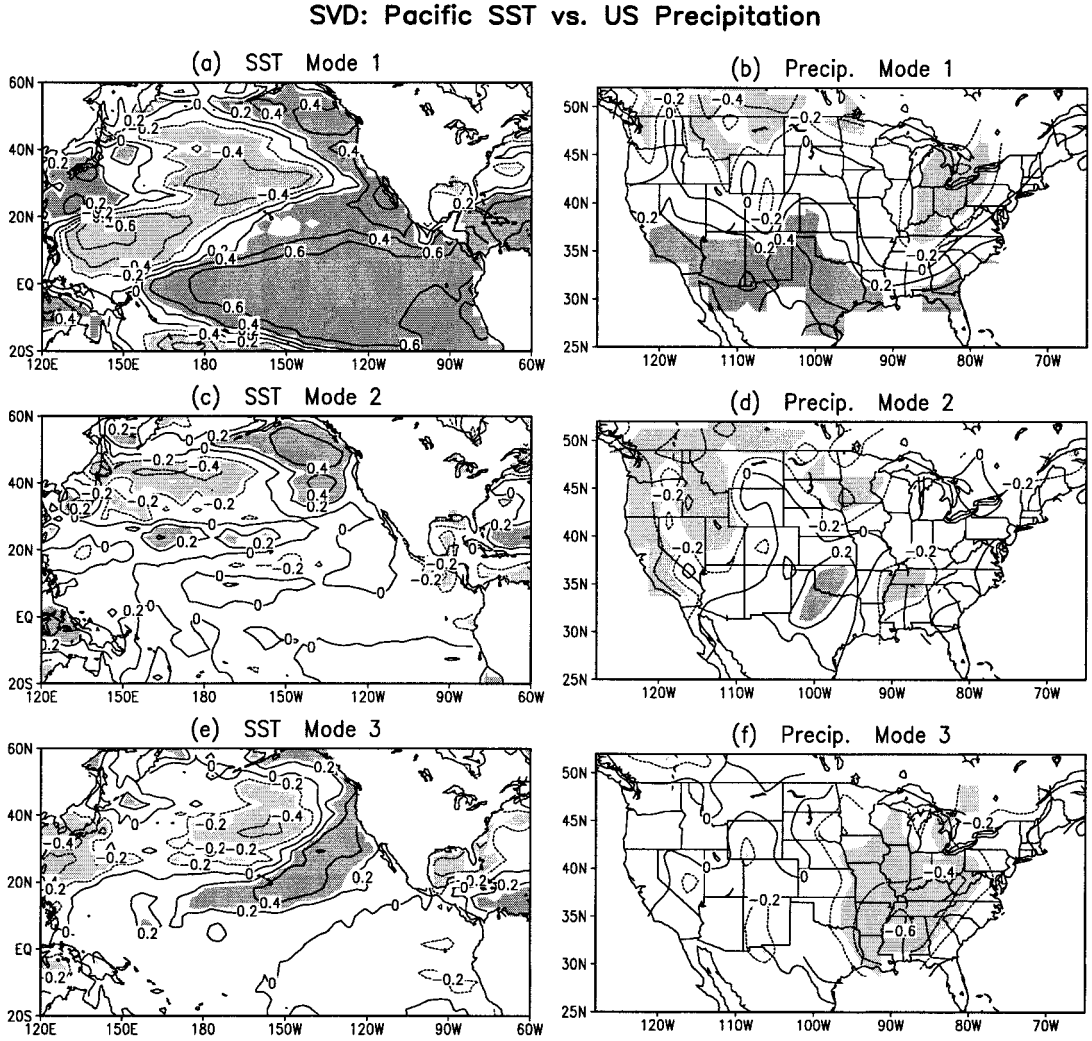

FIG. 2. Heterogeneous correlations of the first three SVD modes between Pacific SST (20°S–60°N) and U.S. precipitation. The contour interval is 0.2 and negative contours are dashed. Dark (light) shadings indicate positive (negative) correlations at the 5% significance level, estimated by the Monte Carlo tests.

11% of the total U.S. precipitation variability, it is important for two reasons. First, this mode is strongly linked to the tropical Pacific SST, thus it possesses potential predictive value. Second, the precipitation variance explained by mode 1 increases significantly when only El Niño and La Niña years are considered. Using 14 yr of El Niño and La Niña events in the 45-yr period, the first mode then accounts for 18% of the U.S. precipitation variance. Given the fact that there is only a small number of strong ENSO years, it is not surprising that the percentage of precipitation variance is relatively low when considering the entire 45-yr record.

The second SVD mode explains 16% of the squared covariance between SST and precipitation. The SST pattern (Fig. 2c) displays a center of positive correlations in the eastern North Pacific and negative correlations in the central and western North Pacific between 40° and 60°N. The precipitation pattern (Fig. 2d) shows large negative correlations in the Pacific Northwest, which contributes to large rainfall variability in this region (Fig. 1b). This mode explains 24% of the precipitation variance, much higher than the first mode, thus indicating a strong association between winter precipitation in the Pacific Northwest and the North Pacific SST.

The third SVD mode (Figs. 2e and 2f) explains 9% of the squared covariance. It shows an out-of-phase relation between rainfall anomalies in the southeastern U.S. and the eastern North Pacific SST and an in-phase relation to the central and western North Pacific SST. Compared to mode 2, positive SST correlations in mode 3 extend southward and westward into the subtropics and negative correlations are shifted toward the east and south in midlatitudes. Significant SST signals are mainly found between 15° and 50°N. The prominent feature in the precipitation field is a broad region of negative correlations spanning across the southeast, the mid–Mississippi River basin, and the Ohio River valley. The pattern is similar to the rainfall anomalies associated with the zonal mean flow fluctuations in Ting et al. (1996, Fig. 10a). The third mode accounts for 12% of the U.S. precipitation variance, which is higher than the ENSO-related mode 1. Similar to the second mode, the third mode indicates a link between U.S. precipitation and North Pacific SST.

The time series of the expansion coefficients for the three SVD modes are shown in Fig. 3. The temporal correlation between the SST and precipitation time series in mode 1 is 0.77, highest among the three modes. The SST time series (Fig. 3a, dark bars) displays large positive and negative fluctuations in El Niño (1957/58, 1972/73, 1982/83, 1986/87, 1987/88, and 1991/92) and La Niña (1955/56, 1970/71, 1973/74, 1975/76, and 1988/89) years, respectively. A trend toward warmer SST starting in 1976/77 winter in the tropical Pacific is also discernible, which has been reported by Trenberth and Hurrell (1994) and Deser and Blackmon (1995). The mode-1 precipitation time series (Fig. 3a, light bars) exhibits consistent fluctuations with the SST in most of the winters, indicating a strong association between the mode-1 precipitation pattern and the El Niño/La Niña SST variation. The two time series show a similar trend after 1990, corresponding to wetter conditions in the Gulf Coast states and California, and drier conditions in the northern part of the United States during recent years. The correlation between the pair of mode-2 time series is 0.69. Both SST and precipitation in mode 2 are dominated by decadal timescale variations. During recent years, the precipitation fluctuations in Fig. 3b are relatively flat and the deviations remain largely positive, consistent with large negative correlations in northern California (Fig. 2d) and prolonged droughts in this region (LeComte 1994). The correlation between the two time series in mode 3 is 0.71. The temporal fluctuations are on timescales shorter than that of mode 2.

It is shown that both tropical and extratropical SSTs tend to accompany prominent U.S. precipitation anomalies. The SVD analysis separates the relation of the U.S. precipitation to the tropical SST from that of the extratropical SST. The large fraction of the squared covariance (64%) and the high-temporal correlation (0.77) between mode-1 SST and precipitation suggest a strong link between the U.S. precipitation and El Niño/La Niña SST variation. The results also show that precipitation anomalies in the two regions of large rainfall variability, that is, the Pacific Northwest and the southeast (Fig. 1b), are often associated with the North Pacific SST anomalies. The former correlate to SST anomalies located between 40° and 60°N (mode 2), and the latter correlate to SST anomalies between 15° and 50°N (mode 3). The SVD analysis indicates that only 10% of the U.S. precipitation variability is related to the tropical SST anomalies, whereas more than 35% of the variability can be linked to the North Pacific SST (Table 1).

It is interesting to contrast the SST–precipitation relations of winter and summer (TW). In both seasons, the relations of U.S. precipitation to tropical SST and to the North Pacific SST are well separated by the SVD analyses. The first SVD mode picks out the ENSO-related precipitation in both seasons, but with distinctive geographic patterns. The strongest rainfall anomalies associated with the tropical SST are located in the northern plains and the Midwest during summer (Fig. 7b in TW), where the tropical SST influence is weakest in winter (Fig. 2b). The covariance between the SST and precipitation (34%) and precipitation variance (7%) explained by the first mode in summer are smaller then those for winter (64% and 11%), indicating stronger tropical SST influence on the U.S. precipitation during winter than summer. Unlike for tropical SST, the precipitation anomalies in the Pacific Northwest and the southeast are related to the North Pacific SST variations in both winter and summer. The total U.S. precipitation variance associated with the North Pacific SST, however, is much larger in winter than in summer (36% vs 10%).

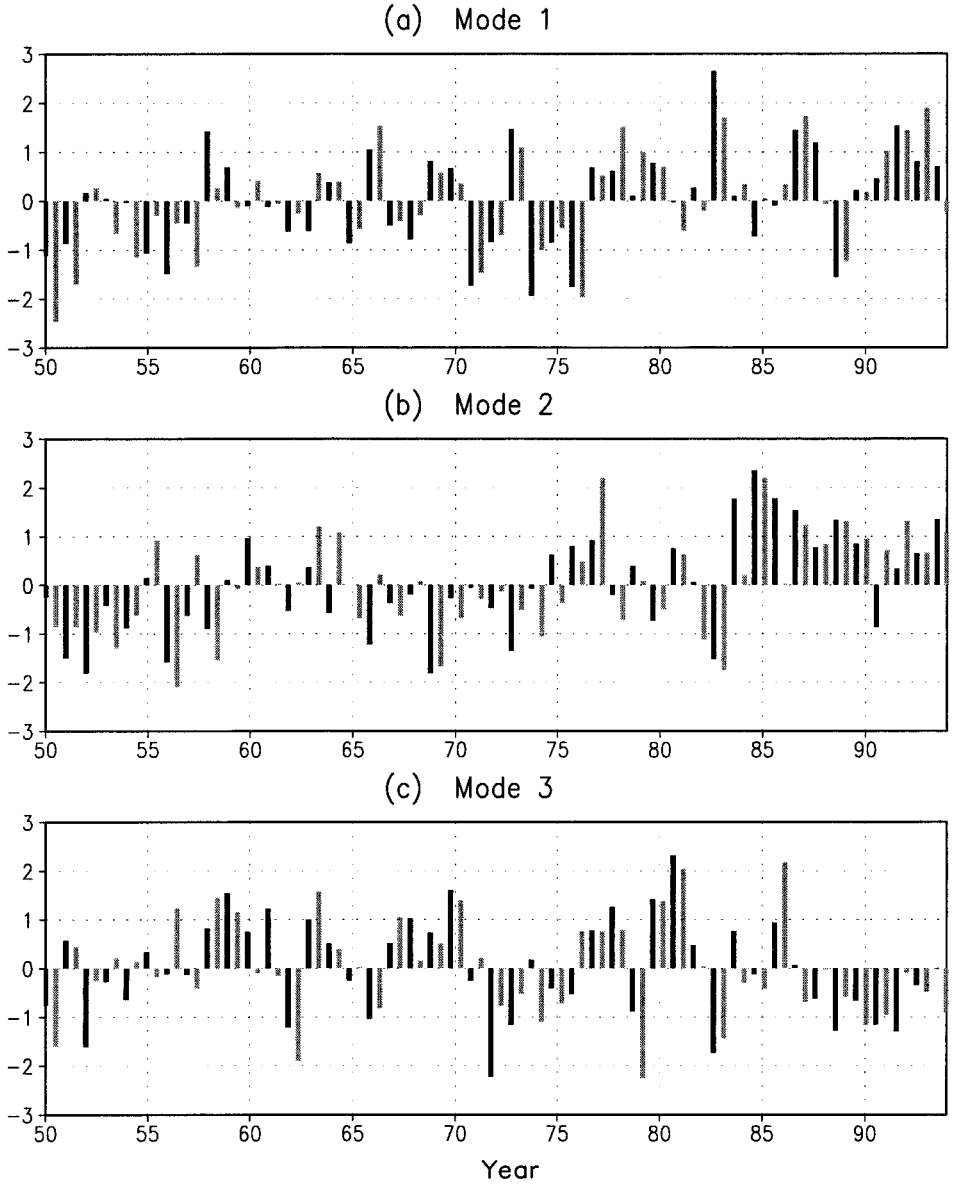

FIG. 3. Normalized time series of the first three SVD modes for Pacific SST (dark bar) and U.S. precipitation (light bar).

c. Associated atmospheric circulation

1) THE 500-MB HEIGHT

To understand the physical processes responsible for the link between the Pacific SST and the U.S. precipitation described above, linear regressions of winter 500-mb height associated with one standard deviation departures of each SVD time series are calculated, as shown in Fig. 4 (contours). For reference, the corresponding North Pacific SST and U.S. precipitation anomalies are shaded in Fig. 4. The height patterns associated with the SST time series (Figs. 4a,c,e) are very similar to those associated with the corresponding precipitation time series (Figs. 4b,d,f). Their resemblance suggests that both Pacific SST and U.S. precipitation in each mode may be linked through the atmospheric circulation.

The 500-mb heights associated with the mode-1 SST and precipitation (Figs. 4a and 4b) exhibit the typical teleconnection pattern associated with the tropical El Niño SST (Horel and Wallace 1981). The circulation associated with warm tropical Pacific SST anomalies is characterized by an anomalous low over the North Pacific, a high over Canada, and an extended low over the southern U.S. Consistent with this circulation, U.S. precipitation is above normal over the Southwest and the Gulf Coast states and below normal along the Northern States. It can be easily infered from Fig. 4 that mode 1

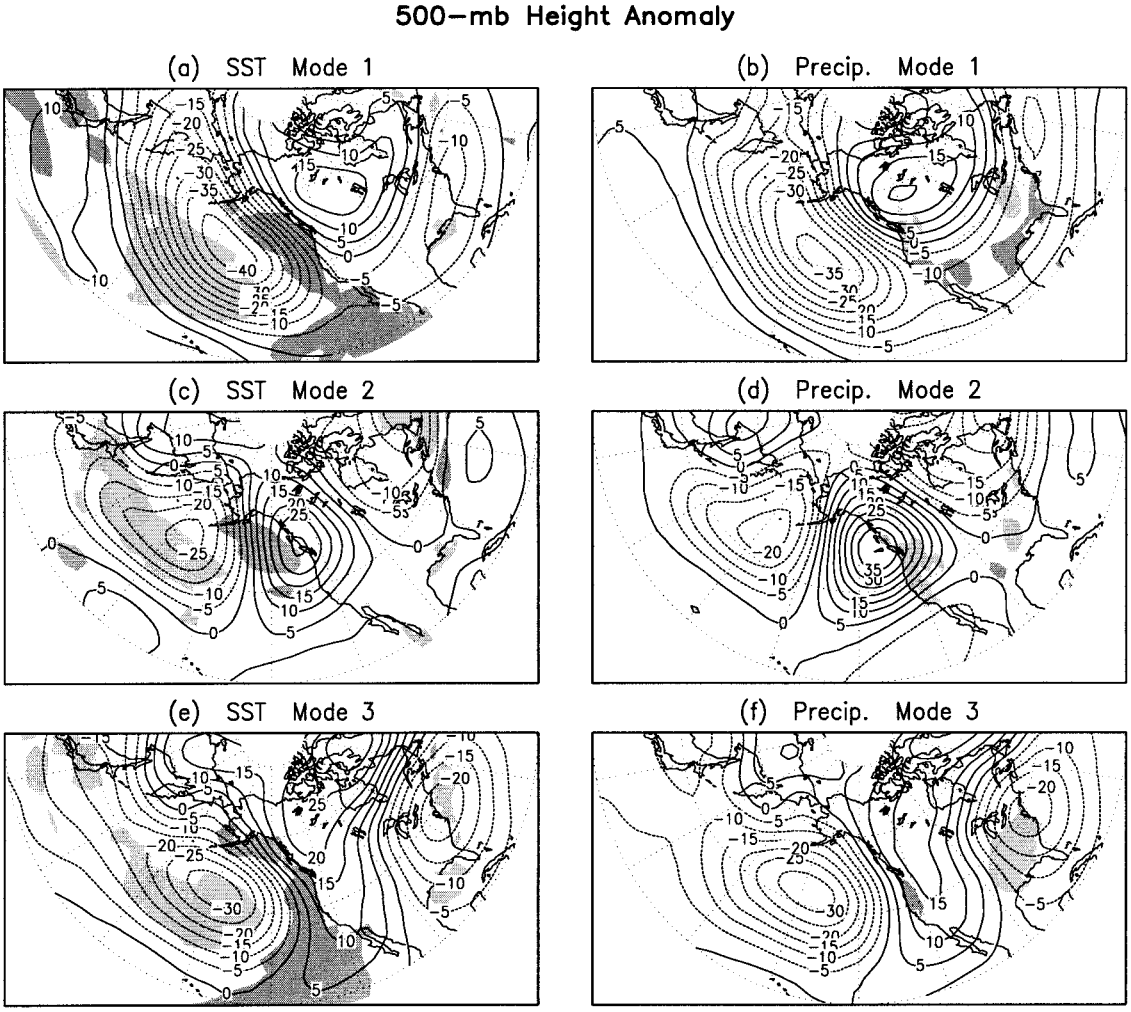

FIG. 4. Regression patterns of 500-mb height (contours), SST (shadings, left), and U.S. precipitation (shadings, right) anomalies associated with one standard deviation departures of the time series of the three leading SVD modes. The contour interval is 5 gpm and negative contours are dashed. SST (precipitation) anomalies below −0.2 K (mm day^{-1}) and above 0.2 K (mm day^{-1}) are indicated by light and dark shadings, respectively.

is associated with zonally elongated westerly anomalies between 20° and 35°N and easterly anomalies around 45°N across the domain. The zonal mean zonal wind is thus increased at lower latitudes and decreased at higher latitudes. The upper-level jet is thereby shifted toward the south. The southward shifted Pacific and U.S. jets are consistent with reduced winter storm activity and precipitation to the north and enhanced storm activity and precipitation to the south.

The 500-mb heights associated with mode 2 display an anomalous low over the central North Pacific and a high over the west coast of North America (Figs. 4c and 4d). The associated zonal wind anomalies vary their signs across the domain, with enhanced westerlies over the central North Pacific, reduced westerlies over the California coast, and enhanced westerlies over the North Atlantic. The strong offshore flow over the Pacific Northwest and northerly winds across the Canadian border into the northern plains are responsible for the dry conditions observed over the Pacific Northwest associated with mode 2.

The 500-mb heights associated with the third SVD mode show a well-defined wave pattern, with positive height anomalies over western North America and negative anomalies over eastern North Pacific and the western North Atlantic, respectively (Figs. 4e and 4f). The large negative precipitation anomalies over the eastern United States (Fig. 4f) are consistent with strong northerly winds at 500 mb. The circulation pattern suggests a deficiency of moisture transport from the Gulf of Mexico, the main moisture source for precipitation occurring in the eastern United States. It can be seen from Figs. 4e and 4f that the 500-mb circulation exhibits large zonal wind increases around 30°N and zonal wind decreases around 55°N. These wind changes are different from those of the first mode. Ting et al. (1996) found

a winter U.S. precipitation anomaly pattern, similar to mode 3 (Fig. 2f), is determined by the midlatitude zonal mean zonal wind anomalies, which are out of phase at 35° and 55°N and independent of the tropical SST variability. The circulation patterns in Figs. 4e and 4f are consistent with the results of Ting et al. (1996) and further suggest that variations in the midlatitude zonal mean zonal winds are somehow related to the North Pacific SST variability (Fig. 2e). A notable difference in circulation patterns between mode 3 and mode 1 is the meridional wind variation. Strong northerly winds are found over the eastern United States in association with mode 3, while little variation in meridional wind is observed in association with mode 1. The enhanced jet over the Pacific in both modes (Figs. 4a and 4e) are likely responsible for the cold North Pacific SST anomalies.

2) THE SLP AND NORTH PACIFIC SST

To access how the atmospheric circulation interacts with the Pacific SST, Fig. 5 shows the anomalous SLP and SST over the North Pacific, obtained using the same linear regression method described earlier. The SLP pattern associated with the first SVD mode displays an anomalous low pressure extending over the eastern and central North Pacific. Since the surface winds are approximately parallel to the isobars over the ocean, we infer the existence of a strong surface westerly wind over the central North Pacific that can act to cool the ocean surface by increasing the heat and moisture fluxes to the atmosphere (Cayan 1992a,b). Close to the North American coast, there is a southerly wind anomaly due to the zonal surface pressure gradient, which may induce an onshore Ekman transport, thus suppressing the upwelling and warming the oceanic mixed layer. Both the warm and cold SST anomalies in the North Pacific are consistent with the SLP pattern. The result indicates that the ENSO-related North Pacific SST anomalies are likely driven by the atmospheric circulation, consistent with many observational and modeling studies (e.g., Wallace and Jiang 1987; Lau and Nath 1994).

The SLP pattern associated with mode 2 (Figs. 5c and 5d) is quite similar to the corresponding 500-mb height pattern (Figs. 4c and 4d), with a high near the west coast of North America and a low over the central North Pacific. Cold SSTs underly anomalous westerlies over the central North Pacific and warm SSTs underly strong southerlies over the eastern North Pacific. It appears that the North Pacific SST anomalies in mode 2 are also forced by the atmospheric circulation, consistent with the finding of Deser and Blackmon (1995). Since time series of both SST and precipitation in mode 2 (Figs. 3c and 3d) exhibit strong interdecadal variability, which are independent of the tropical SST, the atmospheric forcing of SST anomalies over the North Pacific indicates that the internal variability of the extratropical atmosphere might be a possible source for the interdecadal variability of the North Pacific SST. This was suggested by Miller et al. (1994) using an ocean model.

The SLP patterns associated with the third mode (Figs. 5e and 5f) exhibit a basinwide low pressure center over the North Pacific. The distributions of SLP and SST anomalies are to some extent similar to those associated with mode 1. The result suggests that the extratropical SST anomalies associated with mode 3 are also forced by the atmospheric circulation. On the other hand, the cold and warm SST anomalies establish a SST gradient in the eastern North Pacific. A similar temperature gradient in the lower atmosphere may also be established through local sensible heat fluxes. Due to the thermal wind balance, anomalous surface winds can be generated that are consistent with the large SLP gradient in the same area. Thus, interactions between the extratropical SST and the atmospheric circulation are essential to interpret their relation with the third SVD mode.

4. Summary and discussion

The covariabilities of winter average precipitation over the continental United States and Pacific SST have been examined in this study with particular emphasis on the differences between associations with tropical and extratropical SSTs. The winter mean U.S. precipitation displays a strong geographical dependence. Enhanced seasonal mean precipitation, as well as its variability, is found over the eastern and western U.S. during winter.

The SVD analysis is applied to the 45-yr seasonal mean Pacific SST and U.S. precipitation fields. Their coupled patterns are thus objectively identified. The first SVD mode captures the U.S. precipitation variability linked to tropical ENSO SST variability. The result is consistent with the early findings of Ropelewski and Halpert (1986, 1989). The second and third SVD modes depict the U.S. precipitation variability in the Pacific Northwest and the southeast that are linked to the North Pacific SST anomalies. The two precipitation patterns associated with North Pacific SST anomalies account for more U.S. precipitation variability than that associated with the tropical SST variation. However, when only considering El Niño and La Niña years, the variance explained by the first mode increases significantly. Thus the tropical Pacific SST information may be a useful predictor for the U.S. precipitation during El Niño and La Niña winters. The first SVD mode is dominated by the variations on the interannual timescale, while the second and third modes exhibit the variations on both interannual and decadal timescales.

There is some debate regarding whether precipitation anomalies should be measured as actual deviations from a climatological mean or as anomalies normalized by their standard deviations. While a region may have a weak precipitation anomaly, the same region may ex-

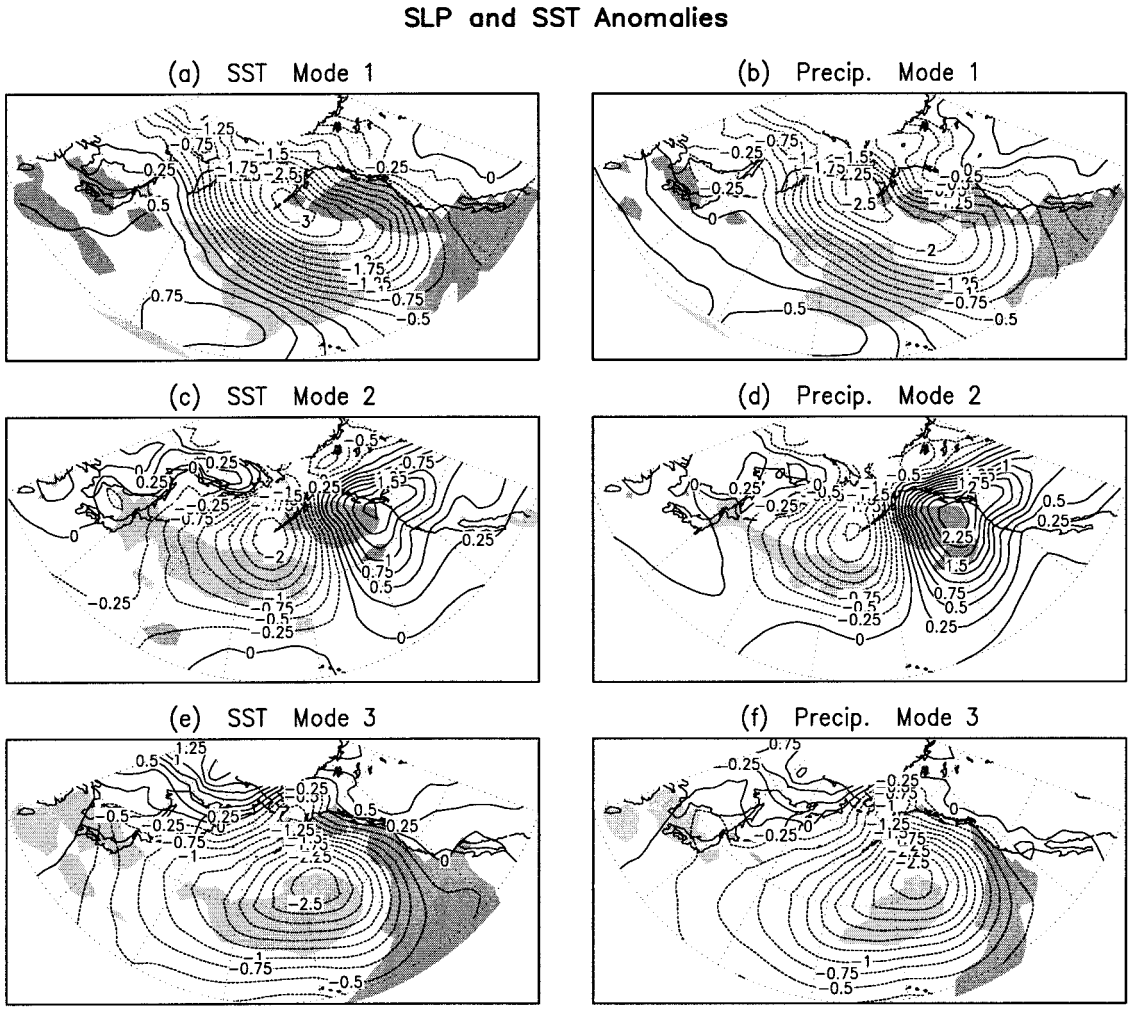

FIG. 5. Regression patterns of SLP (contours) and SST anomalies (shadings) associated with one standard deviation departures of the time series of the three leading SVD modes. The contour interval is 0.25 mb and negative contours are dashed. SST anomalies below −0.2 K and above 0.2 K are indicated by light and dark shadings, respectively.

hibit a large deviation from normal when expressed as a normalized anomaly. In this study, we have examined variations in the actual amount of precipitation, since we are more concerned with regions where aboundant winter mean precipitation occurs. By using normalized precipitation anomalies (not shown), there are no significant changes in the ENSO-related precipitation pattern of SVD mode 1, but some changes in the precipitation patterns associated with the North Pacific SST anomalies. Specifically, the order of mode 2 and mode 3 is interchanged and the significance of the correlations over some regions are slightly reduced (Pacific Northwest) or enhanced (Southwest). In general, the normalized analysis does not qualitatively change the precipitation patterns observed in Fig. 2.

Linear regressions are used to relate the Pacific SST and U.S. precipitation anomalies to the 500-mb height circulation. The precipitation pattern in each SVD mode is associated with a distinct pattern of atmospheric circulation anomalies. The teleconnection pattern in mode 1 is consistent with the atmospheric response to the tropical SST forcing. The first and third SVD modes are associated with large extratropical zonal mean zonal wind anomalies, but having different characteristics. The former is due to the atmospheric response to the tropical SST forcing, while the latter is likely related to extratropical internal atmospheric dynamics that are independent of the tropical SST variability (Ting et al. 1996). The precipitation patterns associated with the first and third modes are similar to those observed in Ting et al. (1996), using regressions against an equatorial SST index and the extratropical zonal wind index, respectively. Unlike the teleconection patterns in the first and third modes, the circulation associated with the second mode shows a more localized feature over the North American west coast. Examining the relations between the North Pacific SST and SLP anomalies suggests that the North Pacific SST anomalies accompa-

nying the U.S. precipitation anomalies in each mode appear largely driven by the atmospheric circulation.

The link between the tropical SST and U.S. precipitation anomalies dominates the covariability between the two fields. The SVD analysis shows, however, that only 10% of the U.S. precipitation variance is accounted for by the tropical SST variations, whereas more than 35% of the precipitation variance is related to the North Pacific SST. This indicates a limitation in the seasonal prediction of the U.S. precipitation based solely on tropical Pacific SST variations. The result also suggests the importance of internal atmospheric processes and possibly extratropical air–sea interaction in determining the winter U.S. precipitation variability. However, the question of how much U.S. precipitation variance is due to the feedback from the North Pacific SST still remains unanswered.

Acknowledgments. We thank the editor and two anonymous reviewers for their constructive comments. We also thank Dr. Robert X. Black for reading the paper and polishing the English writing, which significantly improved the readability of the manuscript. This work was supported by NOAA Grants NA36GPO105 and NA56GPO150 and by the Chinese National Science Foundation.

REFERENCES

Barnston, A. G., 1994: Linear statistical short-term climate predictive skill in the Northern Hemisphere. *J. Climate,* **7,** 1513–1564.

Bretherton, C. S., C. Smith, and J. M. Wallace, 1992: An intercomparison of methods for finding coupled patterns in climate data. *J. Climate,* **5,** 541–560.

Bunkers, J. B., J. R. Miller, and A. T. DeGaetano, 1996: An examination of El Niño–La Niña-related precipitation and temperature anomalies across the Northern Plains. *J. Climate,* **9,** 147–160.

Cayan, D. R., 1992a: Latent and sensible heat flux anomalies over the northern oceans: The connection to monthly atmospheric circulation. *J. Climate,* **5,** 354–369.

——, 1992b: Latent and sensible heat flux anomalies over the northern oceans: Driving the sea surface temperature. *J. Phys. Oceanogr.,* **22,** 859–879.

Deser, C., and M. L. Blackmon, 1995: On the relationship between tropical and North Pacific sea surface temperature variations. *J. Climate,* **8,** 1677–1680.

Higgins, R. W., J. E. Janowiak, and Y. Yao, 1996: A gridded hourly precipitation data base for the United States (1963–1994). *NCEP/Climate Prediction Center ATLAS 1,* U.S. Department of Commerce, 46 pp.

Horel, J. D., and J. M. Wallace, 1981: Planetary-scale atmospheric phenomena associated with the Southern Oscillation. *Mon. Wea. Rev.,* **109,** 813–829.

Hoskins, B., and D. Karoly, 1981: The steady linear response of a spherical atmosphere to thermal and orographic forcing. *J. Atmos. Sci.,* **38,** 1179–1196.

Lau, N.-C., 1985: Modeling the seasonal dependence of the atmospheric response to observed El Niño in 1962–76. *Mon. Wea. Rev.,* **113,** 1970–1996.

——, 1997: Interactions between global SST anomalies and the midlatitude atmospheric circulation. *Bull. Amer. Meteor. Soc.,* **78,** 21–33.

——, and M. J. Nath, 1994: A modeling study of the relative roles of tropical and extratropical SST anomalies in the variability of the global atmosphere–ocean system. *J. Climate,* **7,** 1184–1207.

——, and ——, 1996: The role of the atmospheric bridge in linking tropical Pacific ENSO events to extratropical SST anomalies. *J. Climate,* **9,** 2036–2057.

LeComte, D., 1994: Highlights in the United States. *Weatherwise,* **February/March,** 12–17.

Miller, A. J., D. R. Cayan, T. P. Barnett, N. E. Graham, and J. M. Oberhuber, 1994: Interdecadal variability of the Pacific Ocean: Model response to observed heat flux and wind stress anomalies. *Climate Dyn.,* **9,** 287–302.

Ropelewski, C. F., and M. S. Halpert, 1986: North American precipitation and temperature patterns associated with the El Niño/Southern Oscillation (ENSO). *Mon. Wea. Rev.,* **114,** 2352–2362.

——, and ——, 1989: Precipitation patterns associated with the high index phase of the Southern Oscillation. *J. Climate,* **2,** 268–284.

Smith, T. M., R. W. Reynolds, R. E. Livezey, and D. C. Stokes, 1996: Reconstruction of historical sea surface temperature using empirical orthogonal functions. *J. Climate,* **9,** 1403–1420.

Ting, M., and H. Wang, 1997: Summertime United States precipitation variability and its relation to Pacific sea surface temperature. *J. Climate,* **10,** 1853–1873.

——, M. P. Hoerling, T. Xu, and A. Kumar, 1996: Northern Hemisphere teleconnection patterns during extreme phases of the zonal-mean circulation. *J. Climate,* **9,** 2614–2633.

Trenberth, K. E., and J. W. Hurrell, 1994: Decadal atmosphere–ocean variations in the Pacific. *Climate Dyn.,* **9,** 303–319.

Vose, R. S., R. L. Schmoyer, P. M. Steurer, T. C. Perterson, R. Heim, T. R. Karl, and J. Eischeid, 1992: The global historical climatology network: Long-term monthly temperature, precipitation, sea level pressure, and station pressure data, NDP-041. Carbon Dioxide Information Analysis Center, Oak Ridge National Laboratory, 15 pp. [Available from Carbon Dioxide Information Analysis Center, Oak Ridge National Laboratory, P.O. Box 2008, Oak Ridge, TN 37831.]

Wallace, J. M., and Q.-R. Jiang, 1987: On the observed structure of the interannual variability of the atmosphere/ocean climate system. *Atmospheric and Oceanic Variability,* H. Cattle, Ed., Royal Meteorological Society, 17–43.

——, C. Smith, and C. S. Bretherton, 1992: Singular value decomposition of wintertime sea surface temperature and 500-mb height anomalies. *J. Climate,* **5,** 561–576.

Wang, H., M. Ting, and M. Ji, 1999: Prediction of seasonal mean United States precipitation based on El Niño sea surface temperatures. *Geophys. Res. Lett.,* **26,** 1341–1344.